Benefit of a Sharp Computed Tomography Angiography Reconstruction Kernel for Improved Characterization of Intracranial Aneurysms

Brian O'Meara
Jason P. Rahal, MD
Alexandra Lauric, PhD
Adel M. Malek, MD, PhD

Cerebrovascular and Endovascular Division, Department of Neurosurgery, Tufts Medical Center and Tufts University School of Medicine, Boston, Massachusetts

Correspondence:
Adel M. Malek, MD, PhD,
Department of Neurosurgery,
Tufts Medical Center,
800 Washington Street, #178, Proger 7,
Boston, MA 02111.
E-mail: amalek@tuftsmedicalcenter.org

Received, May 15, 2013.
Accepted, September 5, 2013.
Published Online, September 11, 2013.

Copyright © 2013 by the
Congress of Neurological Surgeons.

BACKGROUND: Computed tomography angiography (CTA) is the first-line imaging modality used for cerebral aneurysms because of its speed and sensitivity for detection, although digital subtraction angiography is often required for more detailed aneurysm shape delineation.

OBJECTIVE: To determine whether a sharper CTA reconstruction kernel can better characterize an aneurysm and improve decision-making before intervention.

METHODS: Fifteen patients presenting with aneurysmal subarachnoid hemorrhage underwent 64-row CTA. CTA data were reconstructed using the default H20f smooth kernel and a H60f sharp kernel and compared with contemporaneous catheter 3-dimensional rotational angiography (3DRA). Aneurysm neck, width, and aspect ratio measurements were made using intensity line plots of identical projections on all imaging datasets and compared by matched-pair statistics.

RESULTS: Aneurysm neck measurements from the H20f smooth kernel revealed overestimation compared with both the sharp kernel (greater by 0.64 $\pm$ 0.21 mm, $P < .01$) and 3DRA (greater by 0.68 $\pm$ 0.19 mm, $P < .01$). There was no statistically significant difference between 3DRA and the sharp kernel CTA measurements. Neck measurements correlated well between the H60f kernel and 3DRA but not between the H20f Kernel and 3DRA (R 0.97 vs 0.86).

CONCLUSION: H60f sharp CTA kernel reconstruction provides more accurate anatomic characterization of cerebral aneurysms than the H20f smooth kernel at the expense of less visually pleasing reconstructions. Because it does not require additional contrast, radiation, or imaging hardware and is more similar to 3DRA, it may aid in selecting the appropriate treatment strategy before to evaluation by catheter-based angiography.

KEY WORDS: 3-D rotational angiography, Aneurysm, Computed tomography angiography, Digital subtraction angiography, Reconstruction kernel, Subarachnoid hemorrhage

Operative Neurosurgery 10:97–105, 2014 DOI: 10.1227/NEU.0000000000000167

Intracranial aneurysms account for 85% of nontraumatic subarachnoid hemorrhage (SAH), which is associated with approximately 50% mortality and significant morbidity.[1] Because as many as 12% of unsecured ruptured aneurysms will rehemorrhage within the first week, rapid detection and evaluation are critical steps in triaging patients to determine treatment either by neurosurgical clipping or endovascular coiling.[2,3]

ABBREVIATIONS: 3DRA, 3-dimensional rotational angiography; **CTA,** computed tomography angiography; **DSA,** digital subtraction angiography; **SAH,** subarachnoid hemorrhage

Computed tomography angiography (CTA) has become the primary method for evaluating intracranial aneurysms.[4-6] The sensitivity and specificity for aneurysm detection with 64-slice computed tomography (CT) approaches that of 2-dimensional digital subtraction angiography (DSA), 3-dimensional rotational angiography (3DRA), and surgical findings and, despite some controversy over its ability to supplant catheter angiography for aneurysm detection, has become widely adopted.[7-11] This finding has been consistent with aneurysms smaller than 3 mm.[6,11] Additionally, CTA has shown to be a valuable adjunct to catheter angiogram–negative nonperimesencephalic SAH.[12] Furthermore, several

Copyright © Congress of Neurological Surgeons. Unauthorized reproduction of this article is prohibited.

studies have assessed the capacity of CTA as the only imaging modality used in the preoperative analysis of patients with ruptured intracranial aneurysms.[13-19] The sensitivity, specificity, and negative predictive value of CTA have suggested it to be a cost-effective initial diagnostic treatment modality despite the advantages of DSA, such as the ability to study cross flow.[11,20-22] Jethwa et al[20] recently analyzed the cost-benefit of using CTA and DSA in the workup of SAH and found that in most centers with modern CT equipment, the sensitivity of CTA was high enough that the additional imaging with DSA was not cost-effective.

However, despite its use as a first-line imaging modality, CTA often lacks the detailed anatomic characterization required to make the decision to treat an aneurysm via an endovascular or open surgical approach, leading to subsequent conventional catheter-based angiography in the majority of cases.

In a preliminary analysis, we found that the use of a sharper CTA kernel has provided more accurate anatomic information that appears closer to catheter-based angiography techniques than smoother CTA kernels at the expense of grainier, less attractive volumetric rendering. CT reconstruction kernels are mathematical functions that selectively enhance the spatial frequency content of the data and determine the trade-off between image sharpness and pixel noise.[23] In this study, we evaluated the ability of an H60f sharp reconstructive kernel to show additional information regarding aneurysm morphology by comparing it with the default H20f smooth kernel and 3DRA to strengthen the potential of using CTA as a primary pretreatment planning study for patients with ruptured intracranial aneurysms.

MATERIALS AND METHODS

Patient Selection and Demographics

All patients presenting with aneurysmal SAH between April 2012 and March 2013 who underwent CTA and contemporaneous catheter angiography were included in the study. Fusiform, mycotic, and extradural aneurysms were excluded. A total of 15 aneurysms from 15 patients (10 men, 5 women; mean age, 61 years; range, 41-88 years) were analyzed. Patient demographics, aneurysm treatment, and location are summarized in Table 1.

TABLE 1. Demographics and Aneurysms[a]

Patient	Sex	Age, y	Location	Treatment
1	M	53	ACOM	Coil
2	F	73	ICA	Coil
3	M	80	ACOM	Clip
4	M	51	BA	Coil
5	M	66	MCA	Clip
6	F	55	ACOM	Clip
7	F	50	PCOM	Coil
8	M	62	PCOM	Coil
9	F	88	MCA	Coil
10	M	41	MCA	Clip
11	F	57	MCA	Coil
12	M	44	ACOM	Coil
13	M	69	PCOM	Clip
14	M	63	MCA	Coil
15	M	57	AChA	Coil

[a]ACOM, anterior communicating artery; ICA, internal carotid artery; BA, basilar artery; MCA, middle cerebral artery; PCOM, posterior communicating artery; AChA, anterior choroidal artery.

CTA and Cerebral Angiography

CTA datasets were acquired using a 64-row multislice CT machine (SOMATOM Definition AS; Siemens Medical Solutions, Malvern, Pennsylvania). Acquisition parameters were 600 mAs, 120 kV, total injection volume of 70 mL iopromide (Ultravist 370; Bayer Health Care Pharmaceuticals, Berlin, Germany), injection rate of 5 mL/s, rotation time of 0.5 seconds, collimation of 0.6 mm, pitch of 0.6, direction caudocranial, and field of view of 180. Reconstruction of the acquired CTA data was done using the default H20f smooth kernel and an H60f sharp kernel. Reconstruction parameters for the smooth kernel included a slice width of 1 mm and an increment of 0.5 mm. For the sharp kernel, a slice width of 0.6 mm and increment of 0.6 mm were used. Axial 512 × 512 matrix slices were used for all analyses.

3DRA data were acquired using a biplane flat-detector DSA system (Axiom Artis; Siemens Medical Solutions). The acquisition was performed using contrast injection of 3 mL/s for 5 seconds with a 1.5-second preinjection delay (Isovue-250; Bracco Imaging SpA, Milano, Italy). The size of each 3DRA data volume was 255 × 255 × 255, with 0.14-mm isotropic voxels. In 1 patient, cone-beam CTA was performed in lieu of 3DRA, using 20-second acquisition while injecting 1 mL/s of contrast with a 2.0-second preinjection delay.

Imaging Analysis

Aneurysm morphology was compared by a line-plot intensity analysis of the edge of the aneurysm at the neck and width to reduce operator bias. First, CTA and angiography volumes were reconstructed using maximum intensity projection multiplanar reconstruction on a Leonardo/Syngo workstation (Siemens AG, Munich, Germany). 3DRA datasets were reconstructed with a 512 × 512 matrix and kernel type HU, with natural fill. Multiplanar reconstructions that best visualized the aneurysms were analyzed with visualization and modeling software (Amira; Visual Sciences Group, Burlington, Massachusetts). The same projection was reconstructed and analyzed with both CTA kernels using the same software workflow. In the Amira analysis software, lines across the aneurysm neck and width (dome) were placed, and image-intensity values along them were plotted along their length. Neck and width edges were calculated as 50% of the maximum value along this plot. The 50% threshold value was chosen because it was consistent with the primary surgeon's estimates of the edge of the aneurysm wall on several trials.

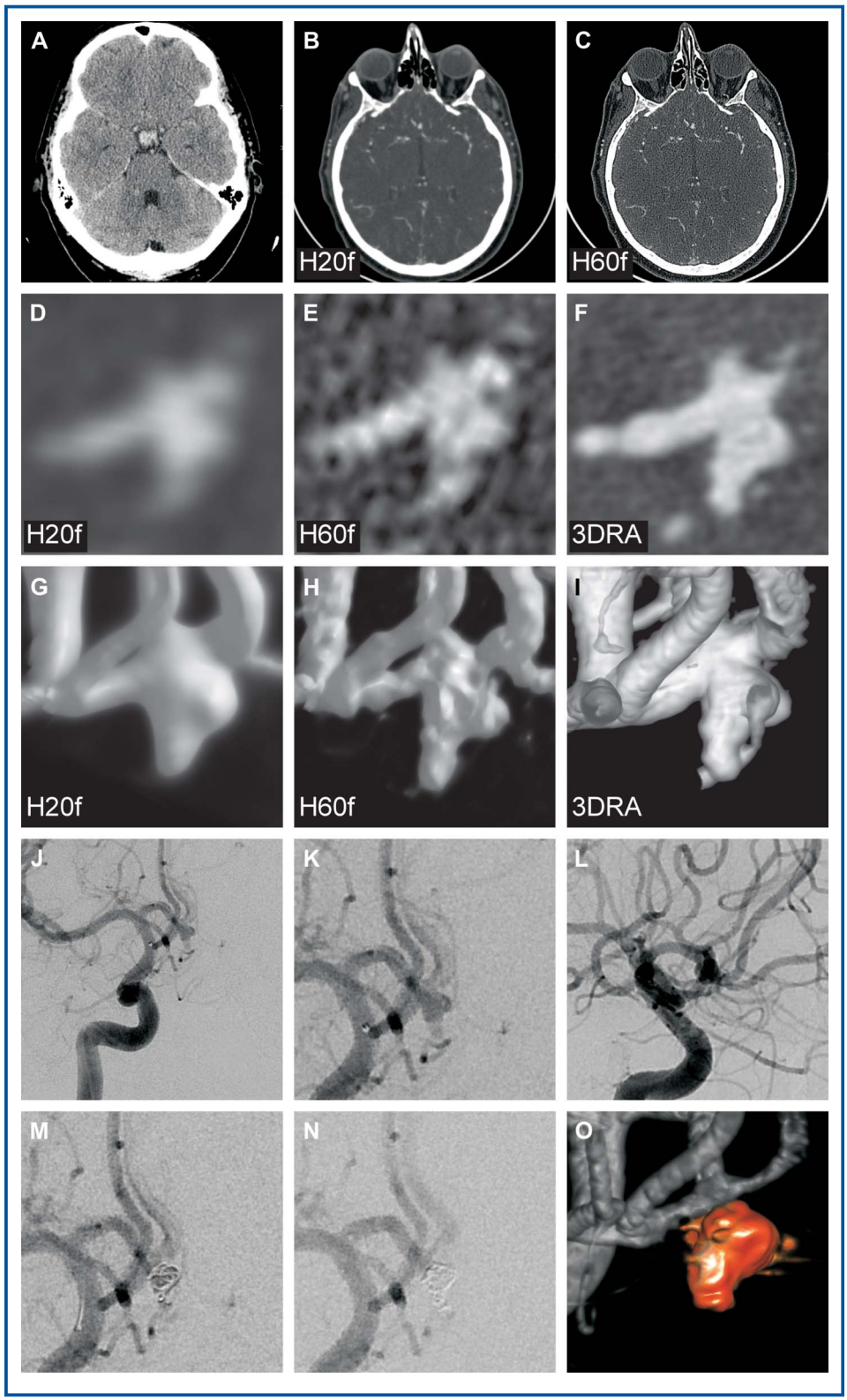
Statistical Analysis

Aneurysm neck and width calculations were analyzed with matched-pair analysis and by linear correlation using JMP statistical software (version 10.0.0; SAS Institute, Cary, North Carolina).

RESULTS

Figure 1 demonstrates a case in which the H60f sharp kernel aided in diagnosis and subsequent management of a patient with

Copyright © Congress of Neurological Surgeons. Unauthorized reproduction of this article is prohibited.



Copyright © Congress of Neurological Surgeons. Unauthorized reproduction of this article is prohibited.

FIGURE 1. *A 44-year-old man presenting with a subarachnoid hemorrhage from an anterior communicating artery aneurysm.* **A**, *presentation axial head computed tomography scan demonstrating a subarachnoid hemorrhage in the suprasellar cistern. Smooth H20f kernel (***B***) and sharp H60f kernel (***C***) axial computed tomography angiography (CTA) through the level of the aneurysm for comparison of overall image quality between the 2 postprocessing techniques. Smooth kernel (***D***) and sharp kernel (***E***) CTA and 3-dimensional rotational angiography (3DRA) (***F***) high-magnification multiplanar reconstructions through the aneurysm. Smooth kernel (***G***) and sharp kernel (***H***) CTA and 3DRA 3-dimensional projections (***I***). Anteroposterior low- (***J***) and high-magnification (***K***) and lateral high-magnification (***L***) digital subtraction angiography depicting the inferiorly pointing anterior communicating artery aneurysm. Anteroposterior digital subtraction angiography after the first coil (***M***) and the final result demonstrating no residual flow in the aneurysm (***N***).* **O**, *3DRA 3-dimensional projection after complete coiling, with coil-pack volume shown in red.*

an anterior communicating artery aneurysm. Qualitatively, images produced by the H60f sharp kernel appear grainy and noisy compared with the H20f smooth kernel (Figures 1B, C). However, the H60f sharp kernel gives a more discrete transition at the aneurysm edge, whereas the H20f smooth kernel exhibited a blurring effect around the edges, best appreciated when viewed at higher magnification (Figures 1D, E). This blurring effect was noted to be particularly significant in areas with sharp angles such as at the neck of the aneurysm. In this case, the smooth kernel depicts a wide neck, with an aneurysm morphology unlikely to be amenable to coil embolization (Figures 1D, G). The H60f sharp kernel, in contrast, suggested a narrow neck (Figures 1E, H). Subsequent 3DRA in this case confirmed a narrow-necked aneurysm, and coil embolization was successful (Figures 1I-O).

Figures 2 and 3 demonstrate the comparison of image quality between the H20f smooth, H60f sharp, and 3DRA reconstructions in a large aneurysm (Figure 2) and a small aneurysm (Figure 3) in high-magnification multiplanar reconstructions. Larger aneurysms, such as the one depicted in Figure 2, do not differ significantly between the different kernels or 3DRA. Figure 3 depicts a small middle cerebral artery aneurysm in an 88-year-old woman presenting with SAH. The H20f smooth kernel reconstruction (Figures 3A, D) demonstrates a small aneurysm with a wide neck. However, on evaluation with the H60f sharp kernel (Figures 3B, E), the neck appears noticeably smaller. Because of this finding, the patient underwent angiography for further characterization of the aneurysm instead of being taken directly to the operating room for microsurgical treatment. The narrow

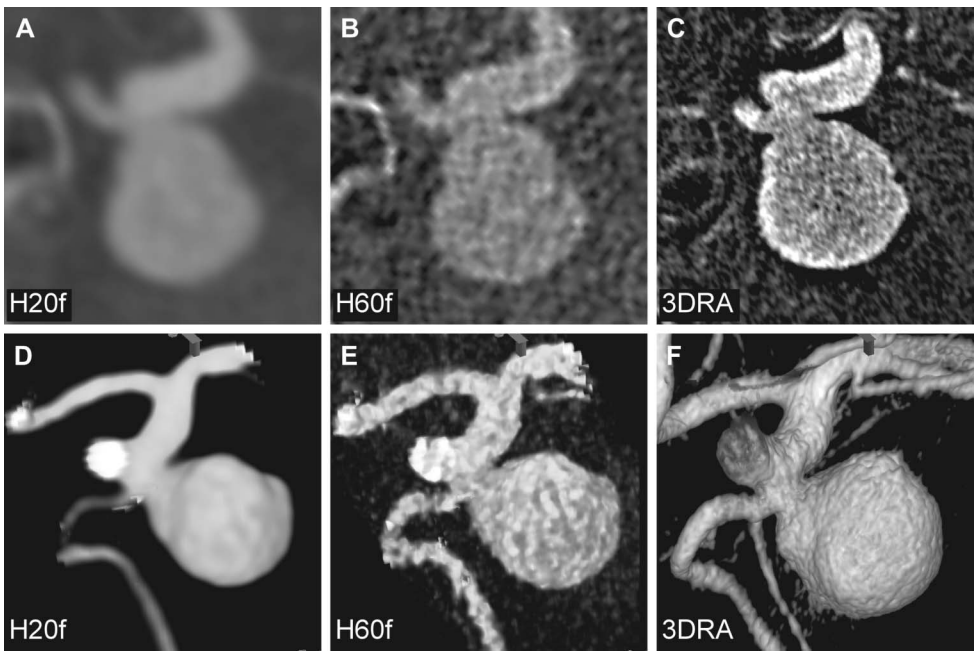


FIGURE 2. *Comparison of imaging modalities of a left posterior communicating artery aneurysm in a 62-year-old man. H20f smooth kernel (***A***) and H60f sharp kernel (***B***) computed tomography angiography (CTA), and 3-dimensional rotational angiography (3DRA) (***C***) multiplanar reconstructions through the aneurysm, oriented for optimal viewing of the neck. H20f smooth kernel (***D***) and H60f sharp kernel (***E***) CTA and 3DRA (***F***) 3-dimensional projections of the aneurysm, again oriented for best visualization of the neck.*

Copyright © Congress of Neurological Surgeons. Unauthorized reproduction of this article is prohibited.

neck was confirmed with angiography (Figure 3G) and, compared with the CTA reconstructions, is even more clearly seen with 3DRA (Figures 3C, F). The patient successfully underwent coil embolization (Figures 3H, I).

Plotting of intensity line probes provides a quantitative visualization of the blurring phenomenon seen with the H20f smooth kernel reconstruction (Figure 4). Although the H60f sharp kernel and 3DRA intensity plots show excellent overlap and nearly indistinguishable steep slopes, the shape of the smooth kernel intensity plot is visibly different with a shallower up- and downgoing slope covering a much wider x-axis range (Figure 4D).

Matched-pair statistical analysis showed that evaluation of the aneurysm neck was particularly sensitive to the reconstruction kernel used (Table 2). The neck size evaluated using the H20f smooth kernel was significantly wider compared with the H60f sharp kernel (3.64 $\pm$ 1.44 vs 3.00 $\pm$ 1.18 mm, $P < .01$). Similarly, compared with 3DRA, the H20f smooth kernel significantly overestimated the neck size (3.64 $\pm$ 1.44 vs 2.96 $\pm$ 1.20 mm, $P < .01$). In contrast, there was no statistical difference between the neck size evaluated using the H60f sharp kernel and the measurements evaluated from the 3DRA data. Linear regression analysis of the H20f smooth and H60f sharp

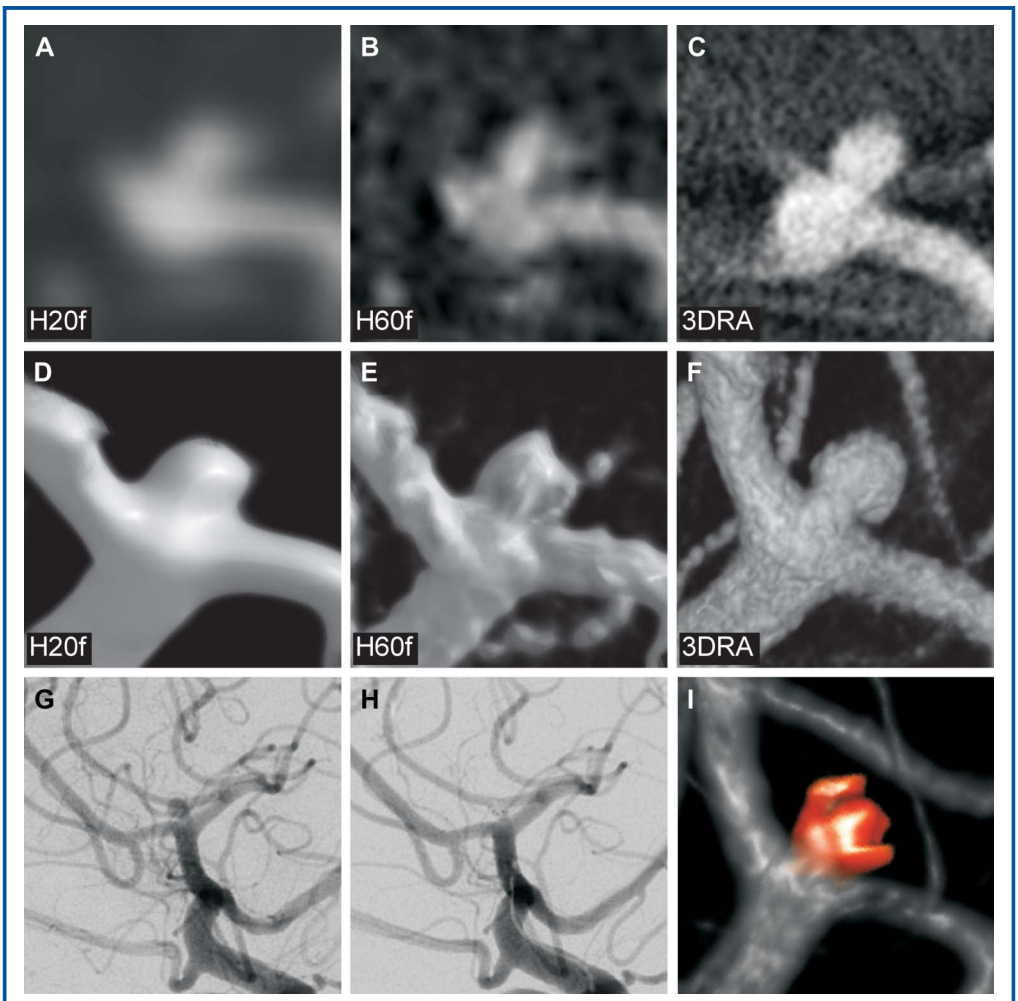


FIGURE 3. *Comparison of imaging modalities of a left middle cerebral artery aneurysm in an 88-year-old woman. H20f smooth kernel (A) and H60f sharp kernel (B) computed tomography angiography (CTA) and 3-dimensional rotational angiography (3DRA) (C) multiplanar reconstructions through the aneurysm, oriented for optimal viewing of the neck. H20f smooth kernel (D) and H60f sharp kernel (E) CTA and 3DRA (F) 3-dimensional projections of the aneurysm, again oriented for best visualization of the neck. G, digital subtraction angiography working view of the aneurysm before coil embolization. H, the same working view after complete coil embolization of the aneurysm. I, 3-dimensional projection of the 3DRA after coil embolization.*

Copyright © Congress of Neurological Surgeons. Unauthorized reproduction of this article is prohibited.

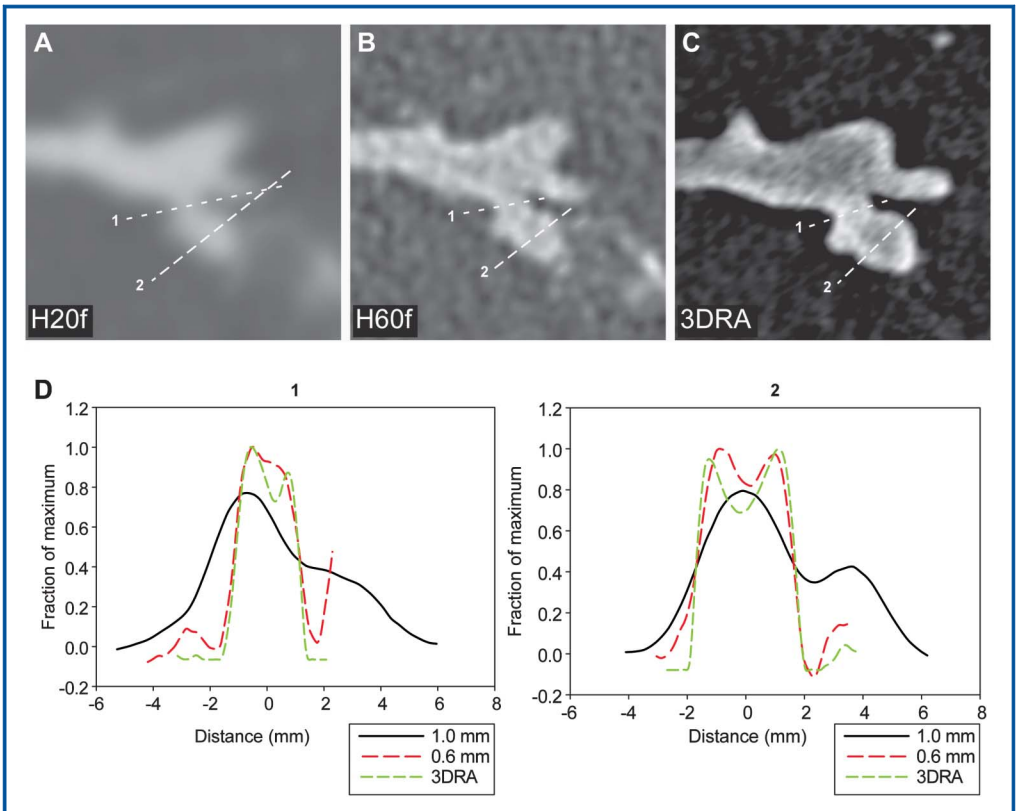


FIGURE 4. *Example of computational analysis of a right internal carotid artery aneurysm in a 73-year-old woman. H20f smooth kernel (A) and H60f sharp kernel (B) computed tomography angiography (CTA) multiplanar reconstructions and 3-dimensional rotational angiography (3DRA) (C) reconstruction, denoting the neck (1) and dome (2) line-plot measurements used in the Amira data analysis software to measure signal intensity for aneurysm edge detection. D, line-plot analysis comparing the neck (1) and dome (2) intensity values for each imaging modality.*

kernels vs 3DRA demonstrated better correlation between the H60f sharp kernel and 3DRA neck measurements (R = 0.97 vs 0.86) (Figure 5). The H20f smooth kernel vs 3DRA regression line demonstrates an upward shift, depicting the increase in neck measurement with the smooth kernel (Figure 5A). Evaluation of the aneurysm width seemed less sensitive to the reconstruction kernel. Although the width size evaluated using the smooth kernel was consistently larger compared with the sharp kernel as well as the 3DRA, these differences did not reach statistical significance.

DISCUSSION

CTA for Evaluation of Cerebral Aneurysms

Although CTA has proved excellent for aneurysm detection, the ability to use CTA for determination of a subsequent treatment modality is not well studied, and typically catheter angiography is used as an additional diagnostic step in all but the most obvious cases. The reason for this is that aneurysm geometry is critical to the determination of whether an aneurysm can be treated by endovascular means or must be treated via a microsurgical approach.[24,25] In particular, the neck size and dome-to-neck ratio (aspect ratio) have been shown to play an important role in this determination.[26-29] The ability to coil an aneurysm is confirmed during attempted embolization using a combination of 2-dimensional DSA and 3DRA. This enables the measurement of aneurysm dimensions and characterization of the parent vessels, small branching arteries, and configuration of the aneurysm geometry. The use of CTA for characterization of an aneurysm is appealing because it may allow better planning and more efficient triaging for subsequent management. Yoon et al[30] demonstrated a significant correlation between analysis of 16-slice CTA data and 3DRA for evaluation of the aspect ratio and small branches near the neck of the aneurysm. However, no study has directly compared the available reconstructive kernels for aneurysm evaluation. Smooth or medium-smooth kernels are most frequently used for aneurysm detection and evaluation.[10,17,31-38] We show here that optimization of the reconstruction of raw CTA data using a kernel with greater sharpness but greater noise may allow for more accurate pretreatment assessment to guide the management of patients presenting with cerebral aneurysms without incurring additional radiation

Copyright © Congress of Neurological Surgeons. Unauthorized reproduction of this article is prohibited.

TABLE 2. Matched-Pair Analysis of Modalities[a]

		Average Distance ± SD, mm		Mean Difference and SE, mm	*P* Value
		Smooth	Sharp		
Smooth (H20f) vs sharp (H60f) kernel	Width	4.24 ± 2.72	4.16 ± 2.82	0.09 ± 0.19	.33
	Neck	3.64 ± 1.44	3.00 ± 1.18	0.64 ± 0.21	.004[b]
	Aspect ratio	1.16 ± 0.40	1.36 ± 0.59	0.21 ± 0.11	.04[b]
		Smooth	3DRA		
Smooth (H20f) kernel vs 3DRA	Width	4.24 ± 2.72	4.15 ± 3.29	0.10 ± 0.24	.35
	Neck	3.64 ± 1.44	2.96 ± 1.20	0.68 ± 0.19	.001[b]
	Aspect ratio	1.16 ± 0.40	1.35 ± 0.65	0.19 ± 0.13	.08
		Sharp	3DRA		
Sharp (H60f) kernel vs 3DRA	Width	4.16 ± 2.82	4.15 ± 3.29	0.01 ± 0.25	.48
	Neck	3.00 ± 1.18	2.96 ± 1.20	0.04 ± 0.08	.29
	Aspect ratio	1.36 ± 0.59	1.35 ± 0.65	0.01 ± 0.08	.44

[a]SD, standard deviation; SE, standard error; 3DRA, 3-dimensional rotational angiography.
[b]Statistically significant data.

exposure or contrast injection, but rather by alternate or supplemental computer reconstruction of the acquired raw data.

Benefit of the Sharp Reconstruction Kernel

A smooth kernel has the effect of smoothing object boundaries and reducing image noise at the expense of reduced image resolution. In contrast, high-pass filters used in sharp convolution kernels preserve higher spatial frequencies, resulting in greater image detail at the expense of greater noise.

In our analysis, the H60f sharp kernel produced images with sharp edges and increased image noise (Figures 2B and 3B), which resulted in jagged 3-dimensional representations (Figures 2E and 3E). Imaging with the standard H20f smooth CTA kernel has a gradual shading appearance of the aneurysm edge in 2 dimensions (Figures 2A and 3A), resulting in smooth, aesthetically pleasing 3-dimensional images (Figures 2D and 3D). This visualization can be misleading: the smooth kernel images can be interpreted with low certainty, and analytical analysis showed that the smooth kernel consistently overestimated aneurysm measurements, particularity in the neck region, where the blurring can lead to overcompensation of the neck dimensions. This overcompensation was confirmed in that the neck distance is statistically larger with the H20f smooth kernel than both the H60f sharp kernel and 3DRA. This problem is not found when evaluating aneurysm width, likely due to a lack of interference with the parent vessel. Hence, the H20f smooth kernel effectively decreases the width-to-neck ratio and perceived ability to coil the aneurysm. The H60f sharp kernel compared with 3DRA showed that the 2 modalities were not statistically different in terms of the neck and dome measurement.

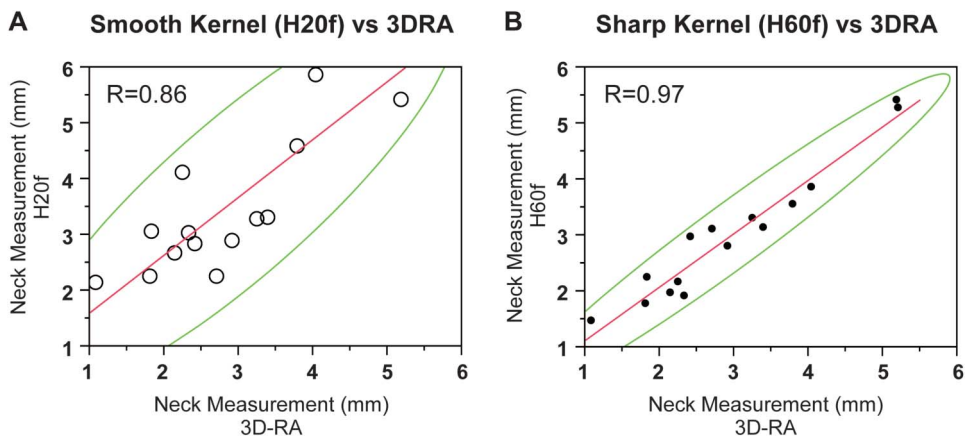


FIGURE 5. *Comparison of neck measurements between smooth and sharp computed tomography angiography (CTA) kernels and 3-dimensional rotational angiography (3DRA).* **A**, *H20f smooth kernel vs 3DRA neck.* **B**, *H60f sharp kernel vs 3DRA. The red lines denote the linear regression analysis. The green ellipses represent the 95% densities.*

Copyright © Congress of Neurological Surgeons. Unauthorized reproduction of this article is prohibited.

Two important conclusions can be drawn from this analysis. First, as seen with the case outlined in Figures 1 and 3, some aneurysms appear to require microsurgical clipping from evaluation with the smooth kernel, but on investigation with the sharp kernel, a decision may be made to consider coil embolization. The H60f sharp kernel reconstructions demonstrated statistically significant smaller neck and aspect ratio measurements compared with the H20f smooth kernel and thus could shift more patients toward attempts at coil embolization in aneurysms that may have appeared only amenable to clipping. Second, the H60f sharp kernel was both qualitatively and quantitatively closer to the 3DRA imaging than the H20f smooth kernel. This allows for a higher degree of confidence when analyzing the CTA imaging and may help the decision in certain cases to proceed with open surgical treatment.

Future Directions

This study used 64-row multislice CT, which has a spatial resolution superior to that of scanners with lower numbers of row detectors, such as 4- or 16-slice CT units[9]; 320-row detectors have since become available. The sharp and smooth kernel reconstructions evaluated here may have variable application to other detector configurations, although the underlying principle of acquisition is the same.

Because of the retrospective nature of the study, we were unable to analyze whether use of the different CTA kernels and 3DRA resulted in changes in treatment strategy or patient outcome. Although the 2 highlighted cases do point toward our experience with the clinical utility of these cases, a prospective, blinded study of treatment and outcome could further the understanding of the differences in these imaging modalities.

The reconstruction of CTA data also has implications for the analysis of rupture risk. A number of studies have identified the importance of the shape characteristics of cerebral aneurysms, such as aneurysm angle and height/width and height/neck ratios in the assessment of rupture risk using CTA.[39-42] These analyses would be highly sensitive to variations in aneurysm shape resulting from the filtering characteristics of the particular reconstruction kernel used in CTA.

CONCLUSION

The H60f sharp CTA reconstructive kernel is superior to the H20f smooth kernel for the characterization of cerebral aneurysms. It is more comparable to catheter-based 3DRA than the H20f smooth kernel and may allow for improved decision-making ability. Inclusion of the H60f sharp kernel in hospital protocol for imaging workup of an aneurysm may increase the clinical utility of CTA without additional radiation or contrast exposure, and with minimal processing time and additional resources.

Disclosure

Dr Malek has received unrestricted research funding from Codman Neurovascular, Microvention Inc, Stryker Neurovascular, Siemens Inc, Ansys Inc, and CD-Adapco for research that is unrelated to this work. The authors have no personal financial or institutional interest in any of the drugs, materials, or devices described in this article. This work was supported by a grant from the National Institutes of Health (NIH-R21HL102685).

REFERENCES

1. van Gijn J, Rinkel GJ. Subarachnoid haemorrhage: diagnosis, causes and management. *Brain*. 2001;124(pt 2):249-278.
2. Inagawa T, Kamiya K, Ogasawara H, Yano T. Rebleeding of ruptured intracranial aneurysms in the acute stage. *Surg Neurol.* 1987;28(2):93-99.
3. Rosenorn J, Eskesen V, Schmidt K, Ronde F. The risk of rebleeding from ruptured intracranial aneurysms. *J Neurosurg.* 1987;67(3):329-332.
4. Chen W, Yang Y, Xing W, Qiu J, Peng Y. Application of multislice computed tomographic angiography in diagnosis and treatment of intracranial aneurysms. *Clin Neurol Neurosurg.* 2010;112(7):563-571.
5. Westerlaan HE, van Dijk JM, Jansen-van der Weide MC, et al. Intracranial aneurysms in patients with subarachnoid hemorrhage: CT angiography as a primary examination tool for diagnosis—systematic review and meta-analysis. *Radiology*. 2011;258(1):134-145.
6. Xing W, Chen W, Sheng J, et al. Sixty-four-row multislice computed tomographic angiography in the diagnosis and characterization of intracranial aneurysms: comparison with 3D rotational angiography. *World Neurosurg.* 2011;76(1-2):105-113.
7. MacKinnon AD, Clifton AG, Rich PM. Acute subarachnoid haemorrhage: is a negative CT angiogram enough? *Clin Radiol.* 2013;68(3):232-238.
8. Kallmes DF, Layton K, Marx WF, Tong F. Death by nondiagnosis: why emergent CT angiography should not be done for patients with subarachnoid hemorrhage. *AJNR Am J Neuroradiol.* 2007;28(10):1837-1838.
9. Li Q, Lv F, Li Y, Luo T, Li K, Xie P. Evaluation of 64-section CT angiography for detection and treatment planning of intracranial aneurysms by using DSA and surgical findings. *Radiology*. 2009;252(3):808-815.
10. McKinney AM, Palmer CS, Truwit CL, Karagulle A, Teksam M. Detection of aneurysms by 64-section multidetector CT angiography in patients acutely suspected of having an intracranial aneurysm and comparison with digital subtraction and 3D rotational angiography. *AJNR Am J Neuroradiol.* 2008;29(3):594-602.
11. Zhang H, Hou C, Zhou Z, Zhang H, Zhou G, Zhang G. Evaluating of small intracranial aneurysms by 64-detector CT angiography: a comparison with 3-dimensional rotation DSA or surgical findings. *J Neuroimaging.* 2012.
12. Delgado Almandoz JE, Jagadeesan BD, Refai D, et al. Diagnostic yield of computed tomography angiography and magnetic resonance angiography in patients with catheter angiography-negative subarachnoid hemorrhage. *J Neurosurg.* 2012;117(2):309-315.
13. Chen W, Yang Y, Xing W, et al. Applications of multislice CT angiography in the surgical clipping and endovascular coiling of intracranial aneurysms. *J Biomed Res.* 2010;24(6):467-473.
14. Agid R, Lee SK, Willinsky RA, Farb RI, terBrugge KG. Acute subarachnoid hemorrhage: using 64-slice multidetector CT angiography to "triage" patients' treatment. *Neuroradiology*. 2006;48(11):787-794.
15. Boet R, Poon WS, Lam JM, Yu SC. The surgical treatment of intracranial aneurysms based on computer tomographic angiography alone—streamlining the acute management of symptomatic aneurysms. *Acta Neurochir (Wien).* 2003;145(2):101-105; discussion 105.
16. Farsad K, Mamourian AC, Eskey CJ, Friedman JA. Computed tomographic angiography as an adjunct to digital subtraction angiography for the pre-operative assessment of cerebral aneurysms. *Open Neurol J.* 2009;3:1-7.
17. Westerlaan HE, Gravendeel J, Fiore D, et al. Multislice CT angiography in the selection of patients with ruptured intracranial aneurysms suitable for clipping or coiling. *Neuroradiology*. 2007;49(12):997-1007.
18. Dehdashti AR, Rufenacht DA, Delavelle J, Reverdin A, de Tribolet N. Therapeutic decision and management of aneurysmal subarachnoid haemorrhage based on computed tomographic angiography. *Br J Neurosurg.* 2003;17(1):46-53.
19. Hoh BL, Cheung AC, Rabinov JD, Pryor JC, Carter BS, Ogilvy CS. Results of a prospective protocol of computed tomographic angiography in place of catheter angiography as the only diagnostic and pretreatment planning study for cerebral aneurysms by a combined neurovascular team. *Neurosurgery*. 2004;54(6):1329-1340; discussion 1340-1322.

Copyright © Congress of Neurological Surgeons. Unauthorized reproduction of this article is prohibited.

20. Jethwa PR, Punia V, Patel TD, Duffis EJ, Gandhi CD, Prestigiacomo CJ. Cost-effectiveness of digital subtraction angiography in the setting of computed tomographic angiography negative subarachnoid hemorrhage. *Neurosurgery*. 2013; 72(4):511-519.
21. Wang H, Li W, He H, Luo L, Chen C, Guo Y. 320-detector row CT angiography for detection and evaluation of intracranial aneurysms: comparison with conventional digital subtraction angiography. *Clin Radiol.* 2013;68(1):e15-e20.
22. Chen W, Wang J, Xing W, et al. Accuracy of 16-row multislice computerized tomography angiography for assessment of intracranial aneurysms. *Surg Neurol.* 2009;71(1):32-42.
23. Weiss KL, Cornelius RS, Greeley AL, et al. Hybrid convolution kernel: optimized CT of the head, neck, and spine. *AJR Am J Roentgenol.* 2011;196(2):403-406.
24. Rahal JP, Malek AM. Clip occlusion versus coil embolization for the treatment of cerebral aneurysms. *J Neurosurg Sci.* 2012;56(3):175-190.
25. Weir B, Amidei C, Kongable G, et al. The aspect ratio (dome/neck) of ruptured and unruptured aneurysms. *J Neurosurg.* 2003;99(3):447-451.
26. Debrun GM, Aletich VA, Kehrli P, et al. Aneurysm geometry: an important criterion in selecting patients for Guglielmi detachable coiling. *Neurol Med Chir (Tokyo).* 1998;38(suppl):1-20.
27. Quasar Grunwald I, Molyneux A, Kuhn AL, Watson D, Byrne JV. Influence of coil geometry on intra-aneurysmal packing density: evaluation of a new primary wind technology. *Vasc Endovascular Surg.* 2010;44(4):289-293.
28. Kiyosue H, Tanoue S, Okahara M, et al. Anatomic features predictive of complete aneurysm occlusion can be determined with three-dimensional digital subtraction angiography. *AJNR Am J Neuroradiol.* 2002;23(7):1206-1213.
29. Brinjikji W, Cloft HJ, Kallmes DF. Difficult aneurysms for endovascular treatment: overwide or undertall? *AJNR Am J Neuroradiol.* 2009;30(8):1513-1517.
30. Yoon DY, Lim KJ, Choi CS, Cho BM, Oh SM, Chang SK. Detection and characterization of intracranial aneurysms with 16-channel multidetector row CT angiography: a prospective comparison of volume-rendered images and digital subtraction angiography. *AJNR Am J Neuroradiol.* 2007;28(1):60-67.
31. Goddard AJ, Tan G, Becker J. Computed tomography angiography for the detection and characterization of intra-cranial aneurysms: current status. *Clin Radiol.* 2005;60(12):1221-1236.
32. Gölitz P, Struffert T, Knossalla F, et al. Angiographic CT with intravenous contrast injection compared with conventional rotational angiography in the diagnostic work-up of cerebral aneurysms. *AJNR Am J Neuroradiol.* 2012;33(5): 982-987.
33. Karamessini MT, Kagadis GC, Petsas T, et al. CT angiography with three-dimensional techniques for the early diagnosis of intracranial aneurysms. Comparison with intra-arterial DSA and the surgical findings. *Eur J Radiol.* 2004;49(3):212-223.
34. Papke K, Kuhl CK, Fruth M, et al. Intracranial aneurysms: role of multidetector CT angiography in diagnosis and endovascular therapy planning. *Radiology*. 2007; 244(2):532-540.
35. Romijn M, Gratama van Andel HA, van Walderveen MA, et al. Diagnostic accuracy of CT angiography with matched mask bone elimination for detection of intracranial aneurysms: comparison with digital subtraction angiography and 3D rotational angiography. *AJNR Am J Neuroradiol.* 2008;29(1): 134-139.
36. Struffert T, Doelken M, Adamek E, et al. Flat-detector computed tomography with intravenous contrast material application in experimental aneurysms: comparison with multislice CT and conventional angiography. *Acta Radiol.* 2010;51(4):431-437.
37. Villablanca JP, Achiriolaie A, Hooshi P, et al. Aneurysms of the posterior circulation: detection and treatment planning using volume-rendered three-dimensional helical computerized tomography angiography. *J Neurosurg.* 2005; 103(6):1018-1029.
38. Zhang LJ, Wu SY, Niu JB, et al. Dual-energy CT angiography in the evaluation of intracranial aneurysms: image quality, radiation dose, and comparison with 3D rotational digital subtraction angiography. *AJR Am J Roentgenol.* 2010;194(1): 23-30.
39. Prestigiacomo CJ, He W, Catrambone J, et al. Predicting aneurysm rupture probabilities through the application of a computed tomography angiography-derived binary logistic regression model. *J Neurosurg.* 2009;110(1):1-6.
40. Ma B, Harbaugh RE, Raghavan ML. Three-dimensional geometrical characterization of cerebral aneurysms. *Ann Biomed Eng.* 2004;32(2):264-273.
41. Hoh BL, Sistrom CL, Firment CS, et al. Bottleneck Factor and height-width ratio: association with ruptured aneurysms in patients with Multiple cerebral aneurysms. *Neurosurgery*. 2007;61(4):716-723.
42. Raghavan ML, Ma B, Harbaugh RE. Quantified aneurysm shape and rupture risk. *J Neurosurg.* 2005;102(2):355-362.

COMMENTS

This paper highlights the limitations of current CTA protocols in which the smoother images at soft CTA kernels may lead to unreliable information when it comes to the question of "clipping vs coiling." Although retrospective, the study makes a case for inclusion of sharp kernels in CTA protocols. Because "soft" and "sharp" kernels may vary with manufacturers and software, indirectly the information also emphasizes the continued importance of catheter angiography as the most reliable technique in assessing aneurysms.

Shah-Naz H. Khan
Columbus, Georgia

This is an excellent and important addition to the literature. The widespread use of 3-dimensional (3-D) CT angiography as a tool to identify cerebral aneurysms most appropriate for surgical ligation or endovascular treatment is recent. Reconstruction is now enabled by complex software programs and high-speed processors. When reconstructing 3-D images, there is always a trade-off between resolution and a realistic depiction of the aneurysm and adjacent blood vessels. This paper explains why many 3-D images do not correlate with the 2-dimensional angiographic images and do not always correlate with the anatomy seen at the time of craniotomy.

When treating patients with cerebral aneurysms, the authors noted that 3-D reconstruction of CTA datasets resulted in an overestimation of aneurysm neck size, and, thus, erroneous dome-to-neck ratio calculations. They studied imaging datasets from CTA on 15 patients. They analyzed these datasets with 2 modes; the standard H20f mode was compared with a higher analysis mode, H60f. In the latter, the edge effects are enhanced. The 3-D rotational angiography datasets were obtained using a biplane flat detector digital subtraction angiography system.

The reconstructed images in the H60f mode defined the neck, parent vessel, and aneurysm body in much sharper detail. Although the noise was greater, the information content was clearly improved. Reconstruction using the H20f mode resulted in smoothing of the neck and degraded delineation of the neck, parent vessel, and the aneurysm dome.

I have experienced this problem in my own practice. There is typically a discrepancy between the 3-D reconstructions, the 2-dimensional angiographic images and the anatomy at the time of craniotomy. This paper clearly defines the problem and outlines a solution. This will be very helpful once implemented into any neuroendovascular practice.

Lee R. Guterman
Amherst, New York

Copyright © Congress of Neurological Surgeons. Unauthorized reproduction of this article is prohibited.